

Contents lists available at ScienceDirect

Journal of Catalysis

journal homepage: www.elsevier.com/locate/jcat



Tuning the ethylene-to-propylene ratio in methanol-to-olefins catalysis on window-cage type zeolites



Zhichen Shi, Aditya Bhan*

Department of Chemical Engineering and Materials Science, University of Minnesota, Minneapolis, MN 55455, USA

ARTICLE INFO

Article history: Received 1 September 2020 Revised 5 January 2021 Accepted 12 January 2021 Available online 30 January 2021

Keywords:
Methanol-to-olefins
Ethylene-to-propylene ratio
Hydrocarbon pool
Small pore zeolites
Transient analysis
Light olefin selectivity

ABSTRACT

Decreasing inlet methanol partial pressure and methanol space velocity during methanol-to-olefins (MTO) catalysis on HSAPO-34, HSSZ-13, and HSSZ-39 increases cumulative ethylene-to-propylene ratio by a factor of ~2.3x, ~2.4x, and ~2.2x, respectively. The composition of hydrocarbons occluded in the catalyst when compared at a similar turnover number during MTO suggests that decreasing methanol concentration in the catalyst bed decreases the extent of methylbenzene homologation within the pool of entrained aromatics, resulting in increments in the concentration of aromatic precursors to ethylene relative to those for propylene. Ethylene-to-propylene ratio changed by a factor of ~1.3x within one catalyst turnover and <10 s on-stream after a step-change in the inlet methanol pressure; in this duration the speciation of entrained methylbenzenes is unchanged as less than 1 mol_C mol_H⁻¹, was converted to hydrocarbons, revealing that instantaneous ethylene and propylene selectivity depends sensitively on local methanol concentration. These mechanistic insights identify local methanol concentration as the salient parameter in modulating product selectivity during MTO on window-cage type materials.

© 2021 Elsevier Inc. All rights reserved.

1. Introduction

Methanol-to-olefins (MTO) conversion on window-cage type zeolite and zeotype catalysts containing large-cages interconnected by narrow windows selectively produces light olefins (C2- $C_4 > 90\%C$) because these microporous materials entrain methylbenzenes as active organic co-catalysts within cavities once engendered, rendering efficient the conversion of methanol to light olefins without "reconstitution" of hydrocarbon pools during MTO [1–5]. These methylbenzenes engage with methanol to selectively yield ethylene and propylene (~80%C) via acid-catalyzed dealkylation reactions [6-11] where ethylene originates from tetra-methylbenzene, and propylene originates from pentamethylbenzene and hexa-methylbenzene [12,13]. While cumulative ethylene and propylene selectivity is high, tuning the relative selectivity of ethylene and propylene remains a challenge during MTO on window-cage type materials where HSAPO-34, a silicoaluminophosphate with CHA topology, is of particular interest because of its industrial relevance [1,14,15].

Material characteristics, the structure or composition of the window-cage type materials, have been the primary focus in prior investigations that detail strategies to control the ethylene-to-

* Corresponding author.

E-mail address: abhan@umn.edu (A. Bhan).

propylene ratio in MTO. Decreasing cage size has been shown to systematically increase ethylene selectivity during methanol conversion where the cage topology and its effect on the degree of methylation of aromatic hydrocarbon species were invoked to rationalize the observed structure-function relationship [16-25]. Inui and co-workers reported ethylene selectivity of ~90%C during MTO on cage-containing metallosilicate and/or metalloaluminophosphates attributing these selectivity characteristics to the substitution of metals of larger ionic radii than Al in the framework resulting in a decrease in the cage size and acid strength of protons [26-28]. Metal exchange in extra-framework positions has also been shown to improve the initial ethylene-to-propylene ratio where ethylene selectivity increases monotonically with increasing Zn content of the catalyst [29–31]. These methods, however, suffer from complicated synthetic protocols that require incorporation of metal ions during synthesis [26–28], insignificant changes in cumulative ethylene selectivity despite improvements in the initial ethylene selectivity [29-31], detrimental effects on catalyst lifetime [29-31], and, limited applicability across window-cage type materials of varying topology [16]. Prior reports that describe the effects of process parameters on ethylene-topropylene ratio on HSAPO-34 where higher reaction temperature and lower inlet methanol partial pressure leads to higher selectivity to ethylene do not justify the origins of the observed increment in ethylene selectivity with decreasing inlet methanol pressure nor

generalize the method to window-cage type materials of different structures [1.14.15.32].

Here, we demonstrate and rationalize on a mechanistic basis a strategy that modulates light olefins selectivity during MTO on window-cage type materials by noting systematic increases in ethylene-to-propylene ratios during MTO on HSAPO-34 and HSSZ-13, both of CHA topology, and HSSZ-39 with AEI topology with decreasing inlet methanol partial pressure and space velocity. Cumulative ethylene-to-propylene ratios trend with changes in the speciation of methylbenzenes entrained within the cavities when compared at similar turnover number and ethylene-to-propylene ratio changes instantly in less than one catalyst turnover (<10 s on-stream) with a step-change in methanol pressure, revealing the critical role of methanol concentration in controlling ethylene and propylene selectivity during MTO on window-cage type materials.

2. Materials and methods

2.1. Material characterization

The detailed characterization for powder X-ray diffraction, N₂ physisorption, scanning electron microscopy, and ammonia temperature-programmed desorption (TPD) of HSAPO-34, HSSZ-13, and HSSZ-39 used in this study has been reported previously [33,34] and is summarized in Table 1. The total number of Brønsted acid sites, determined using NH₃-TPD (SI, Fig. S1.1), was used to calculate space velocity and turnover numbers during methanol conversion. The bulk crystal structure of HSSZ-13, HSAPO-34, and HSSZ-39 matched the known reported structure for CHA and AEI [35], as confirmed by XRD (SI, Fig. S1.2).

2.2. Catalytic testing

All experiments were performed in a tubular glass-lined stainless-steel reactor (6.35 mm O.D. and 4 mm I.D., SGE Analytical Science) placed in a resistively heated furnace (Applied Test Systems). The reaction temperature was measured using a K-type thermocouple (Omega) wrapped around the reactor peripherally with the tip placed at the center of the catalyst bed and was regulated with an electronic controller (Watlow). The catalyst was mixed with sand (subjected prior to an overnight wash in 2 M HNO_3 solution followed by DI water rinse until pH ~ 7, and a final thermal treatment in flowing dry air (1.67 cm³ s⁻¹) at 1273 K (0.083 K $\rm s^{-1}$ ramp rate from room temperature) for 16 h) and the mixture was pre-treated in flowing dry air (1.67 cm³ s⁻¹) at 873 K $(0.0167 \text{ K s}^{-1})$ for 6 h prior to cooling to the desired reaction temperature in helium flow (1.67 $\mbox{cm}^3~\mbox{s}^{-1}$). The composition of the reactant and product streams were quantified using a gas chromatograph (GC, Agilent GC 7890A) equipped with a dimethylpolysiloxane HP-1 column (50 m \times 320 μ m \times 0.52 μ m)

 Table 1

 Physical and chemical characteristics of zeolites used in the study.

	HSSZ-13	HSAPO-34	HSSZ-39
Framework type	СНА	СНА	AEI
BET Surface Area ^a / m ² g ⁻¹	560	554	506
Micropore volume ^a / cm ³ g ⁻¹	0.28	0.28	0.27
H ⁺ density ^b / mmol g ⁻¹	0.55	0.92	0.83
Si/Al or (Al + P)/Si ^c	12.9	10.3	9.0

^a Obtained from N₂ physisorption at 77 K.

connected to a flame ionization detector and a PorapakQ (4.6 m \times 3.2 mm \times 2 mm) connected to a thermal conductivity detector.

Methanol reactions were carried out at sub-complete methanol conversion at 673 K with varying inlet methanol partial pressures and space velocities. Methanol space velocity, defined here as the inlet methanol molar flowrate normalized by the total number of Brønsted acid sites in the catalyst bed, was varied by either varying the total amount of catalyst in the bed or varying the inlet methanol flowrate without changing the inlet methanol composition. Methanol (CHROMASOLV; Honeywell) was fed using a glass syringe (Scientific Glass Engineering) and a syringe pump (Cole Parmer 78-0100C) to heated lines and carried by a gas stream (He (99.999%, Matheson) and Ar (99.9999%, Matheson) as internal standard) whose flow was controlled by mass flow controllers (Brooks 5850E). The conversion was calculated based on the total amount of methanol/ dimethyl ether (DME)-derived carbon atoms observed in the effluent hydrocarbons. Instantaneous product selectivity is defined as the formation rate of a particular product per total product formation rate at a given instant of time (and consequently, a specific turnover number). Cumulative product selectivity is defined as the fractional contribution from formation of a particular product to the total catalyst tunovers [36]. Turnover number, the cumulative amount of methanol/ dimethyl etherderived carbon atoms observed in the effluent hydrocarbons normalized by the number of Brønsted acid sites in the catalyst bed, accounts for the effects of acid site density in the catalyst bed, methanol inlet concentration, and space velocity on reaction progress, and thus, was used to assess reaction progress and evolution of entrained hydrocarbons during methanol conversion [37,38]. During the switching experiment, the reaction was allowed to proceed until product selectivity was noted to be invariant with reaction progress. The flow was then switched instantaneously to a feed with a different methanol partial pressure and space velocity. Transient product evolution during switching experiments was measured with both an online mass spectrometer (MS, MKS Cirrus 200 Quadrupole system, m/z = 4, 27, 31, 41, 40) and a gas chromatograph. GC analysis with high temporal resolution was achieved using a sixteen-position selector (VICI Valco) that can step incrementally to store reactor effluent mixtures at timed intervals (as low as 10 s) for later analysis.

In experiments where the content of the entrained methylbenzenes was of interest, the reaction was quenched rapidly by displacing the resistively heated furnace with desk fans (-8 K s^{-1}) once the turnover number reached $\sim 1000 \text{ mol}_{\text{C}} \text{ mol}_{\text{H}^+}^{-1}$ or at the end of catalyst lifetime (conversion <10 %C) if the total turnover number was less than 1000 mol_{C} $\text{mol}_{\text{H+}}^{-1}$. The catalyst bed was then transferred to a glass vial and suspended in 1 cm³ of 1 M HCl solution (37 wt% HCl; Sigma-Aldrich, ACS Reagent) overnight to effect dissolution of the HSAPO-34 framework. The resulting suspension was neutralized by addition of 1 M NaOH (Sigma-Aldrich, \geq 99.99%) followed by addition of 1 cm³ of CH₂Cl₂ (with ~0.15 wt % C₂Cl₆ (Sigma-Aldrich, 99%) added as an internal standard) for extraction of the liberated organic molecules from the aqueous phase. The speciation of aromatics in the organic layer was then identified using a mass spectrometer (Agilent MSD 5975C) and quantified using a gas chromatograph (Agilent 7890A).

3. Results and discussion

3.1. Effect of inlet methanol pressure and space velocity on ethylene-to-propylene ratio

Fig. 1 shows trends in cumulative ethylene-to-propylene *carbon* ratios $(C_2:C_3)$ with the product of methanol inlet pressures and space velocities during methanol conversion on HSSZ-13 and

 $^{^{\}rm b}$ Cumulative amount of ${\rm NH_3}$ desorbed upon thermal treatment of ${\rm NH_4^+exchanged}$ samples at 823 K.

^c Obtained from energy-dispersive X-ray spectroscopy (EDS) measurements.

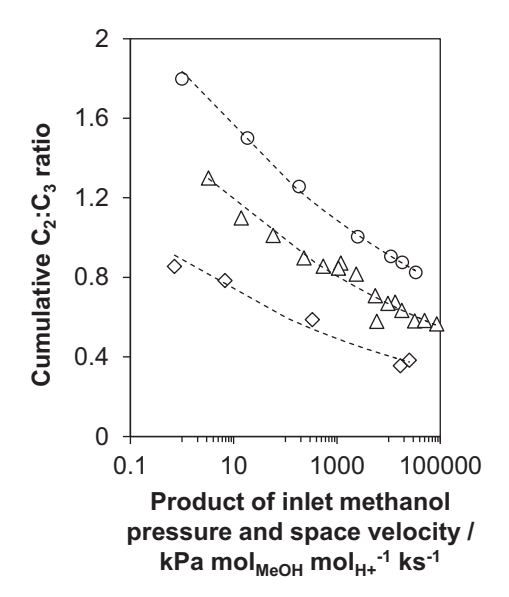


Fig. 1. Cumulative ethylene-to-propylene carbon ratio $(C_2:C_3)$ measured until the end of catalyst lifetime (conversion profiles in SI, Fig. S2.2, S3.1, and S4.1) during methanol-to-olefins conversion on HSSZ-13 (\bigcirc), HSAPO-34 (\triangle), and HSSZ-39 (\diamondsuit) with respect to the product of inlet methanol pressure and space velocity during MTO at sub-complete methanol conversion.

HSAPO-34-silicoaluminates and silicoaluminophosphates of CHA topology—and HSSZ-39, a silicoaluminate of AEI topology, as decrements in either methanol inlet space velocity or partial pressure decrease local methanol concentration-methanol concentration that varies along the length of the catalyst bed and varies with reaction progresses because of the non-differential and transient nature of MTO [36] (instantaneous product selectivity and conversion profiles for all data shown in Fig. 1 are shown in SI, Sections 2-4). Lower ethylene-to-propylene ratios were observed on HSSZ-39 relative to HSSZ-13 or HSAPO-34, consistent with prior reports in the literature [16-24,34] where the topology-dependence of product selectivity has been attributed to effects of spatial confinement on the speciation and stabilization of aromatic precursors to light olefins entrained in the cavities of the catalyst [12,16,17,21,24,25]. Here, we demonstrate that cumulative ethylene selectivity increases with decrements in inlet methanol partial pressure and space velocity irrespective of zeolite topology or chemical composition with the ratio increasing from 0.82 to 1.80, 0.58 to 1.30, 0.36 to 0.85 on HSSZ-13, HSAPO-34, and HSSZ-39, respectively (Fig. 1).

Such dependence of ethylene-to-propylene ratio with inlet methanol pressure and/or space velocity is distinct from that observed on MFI where ethylene selectivity increases monotonically with increasing inlet methanol pressure as increments in methanol pressure increase propagation of the aromatics-based cycle relative to propagation of the olefins-based cycle [38-40]. We surmise that this difference arises from the distinct chemical origins of light olefins in zeolites of different topology where ethylene formation is mechanistically different from propylene and higher olefins during methanol conversion on zeolites of larger channel sizes [10,38,41,42] while methylbenzenes are predominant organic co-catalysts for olefins production during methanol conversion on window-cage type materials [7,32]. The former is supported by isotopic switching experiments with 12C/13Cmethanol feed at steady state on HZSM-5 where the 13Cincorporation of ethylene closely matched that of aromatics while the ¹³C-incorporation of propylene matched that of higher olefins [42]. The concurrent propagation of the aromatics-based and olefins-based cycles for ethylene and propylene production has

also been reported by Hwang et al. [37] at early stages of methanol conversion on HSAPO-34 where co-feeding ¹³C-propylene with ¹²C-dimethyl ether on HSAPO-34 resulted in decrements in ethylene selectivity and increments in butene selectivity with ¹³Ccontent of ethylene distinct from other olefins. Such changes in product selectivity, however, decrease with reaction progress, leading to the conclusion that alkylbenzene precursors and pathways dominate ethylene and propylene production during methanol conversion on HSAPO-34 for a majority of catalyst turnovers [37]. This is consistent with previous reports where Song et al. [7,32] utilized ¹³C MAS NMR spectroscopy to characterize the identity and concentration of entrained organics inside HSAPO-34 and observed that increments in the concentration of methylsubstituted aromatics at later times-on-stream coincided with increasing light olefins yields, affirming the pertinence of polymethylbenzenes as precursors for light olefins formation during methanol conversion on HSAPO-34.

Hwang et al. [13] further employed site-specific isotope tracing experiments to distinguish between isotope labels in aromatic rings versus aromatic methyl positions and concluded that tetramethylbenzene undergoes dealkylation via the side-chain mechanism to yield ethylene while penta-methylbenzene and hexamethylbenzene undergo dealkylation via the pairing mechanism to vield propylene during MTO on HSAPO-34. This mechanistic conclusion was corroborated by Ferri et al. [12,25] who reported increasing propylene-to-ethylene ratios with increasing cavity size of window-cage type materials and related this observation to an increasing degree of methylation of entrained methylbenzenium cations formed in the paring mechanism exploiting a combination of DFT calculations and ¹³C NMR spectroscopy. We postulate that the trends between cumulative ethylene-to-propylene ratio and inlet methanol pressure and space velocity may be related to changes in the extent of homologation within entrained methylbenzenes as methanol concentration local to organic co-catalysts decreases with decreasing inlet methanol partial pressure and space velocity where lower methanol concentration increases the concentration of tetra-methylbenzene relative to that of pentaand hexa-methylbenzene. We probed this hypothesis by analyzing the independent effects of inlet methanol partial pressure and space velocity on entrained methylbenzene speciation and product selectivity during MTO on HSAPO-34 (see Section 3.2).

Fig. 2a shows the profiles of instantaneous ethylene-topropylene ratio with turnover number during MTO on HSAPO-34 with varying inlet methanol partial pressures (product selectivities as a function of time-on-stream are shown in detail for each methanol inlet pressure in Fig. S2.1). Ethylene-to-propylene ratio, irrespective of inlet methanol partial pressure, is low at early catalyst turnovers and increases as the reaction progress (Fig. 2a) as a consequence of the increased relative propagation of the aromatics-based cycle with respect to the olefins-based cycle (vide supra) [7,8,37]. The product selectivity and ethylene-to-propylene ratio eventually plateau (Fig. 2a), suggesting that the provenance of light olefins does not change with reaction progress or catalyst deactivation once the hydrocarbon pool matures [37] (conversion profiles shown in Fig. S2.2). Decrements in the inlet methanol partial pressure, however, decrease the rate of methanol-induced hydrogen transfer [36,38,43,44], resulting in (i) preferential propagation of the olefins-based cycle relative to the aromatics-based cycle at early turnovers [37,45], and (ii) decrements in rates of aromatic homologation and of molecular events prescribing maturation of the hydrocarbon pool. These, taken together, contribute to the lower initial ethylene-to-propylene ratio, as reflected by larger catalyst turnovers being required prior to achieving product selectivity that remains invariant with reaction progress, during MTO on HSAPO-34 with lower inlet methanol partial pressures (Fig. 2a). Despite lower initial ethylene-to-propylene ratios during

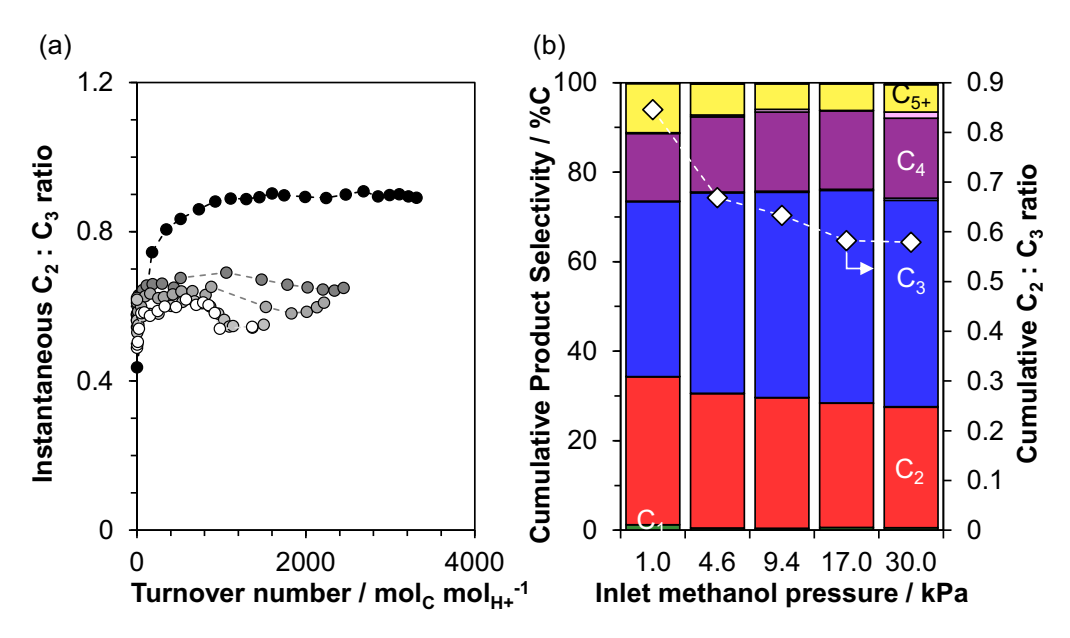


Fig. 2. (a) Instantaneous ethylene-to-propylene carbon ratio $(C_2:C_3)$ versus turnover number, and (b) cumulative product selectivity (bar, *left ordinate*) and cumulative $C_2:C_3$ ratio $(\diamondsuit, right \ ordinate)$ when compared at ~1300 mol $_C$ mol $_H^{-1}$ turnover number during methanol-to-olefins conversion on HSAPO-34 at 673 K, methanol space velocity of ~1200 mol $_C$ mol $_H^{-1}$ ks $^{-1}$ and methanol pressures of 1.0 (\bullet), 4.6 (\bullet), 9.4 (\bullet), 17.0 (\bullet), 30.0 kPa (\circ). The dark- and light-shaded bars represent the olefinic and paraffinic forms, respectively, of the respective carbon group listed in the dark bars.

MTO with lower inlet methanol pressure, the cumulative ethylene-to-propylene ratio increases monotonically from 0.58 to 0.85 during MTO on SAPO-34 with decreasing inlet methanol pressure from 30 kPa to 1 kPa when compared at a similar turnover number (Fig. 2b, Fig. S2.1). Such changes in product selectivity were obtained while maintaining high olefins selectivity (>80%C towards C_2 - C_4 olefin; Fig. 2b, Fig. S2.1).

Fig. 3 shows the trends of cumulative ethylene-to-propylene ratio with methanol space velocity where ethylene-to-propylene ratio increases by a factor of ~1.4x with methanol space velocities decreasing from 2866 to 79 mol_{C} $\text{mol}_{\text{H}^+}^{-1}$ ks⁻¹ at a methanol inlet pressure of 30 kPa, and increases by a factor of ~1.3x with methanol space velocities decreasing from 1192 to $\text{mol}_{\text{C}}^{-1}$ hs⁻¹ to 14

 $\mathrm{mol_C}$ $\mathrm{mol_{H^+}^{-1}}$ $\mathrm{ks^{-1}}$ at a methanol inlet pressure of 1 kPa (detailed instantaneous product selectivity shown in SI, Figs. S2.3 – S2.4). This is consistent with increasing ethylene selectivity with decreasing methanol flowrates during MTO on HSAPO-34 reported by Haw and co-workers [32], who used ¹³C NMR to relate ethylene selectivity to the concentration of xylene and tri-methylbenzenes and propylene selectivity to the concentration of tetra-, penta-, and hexa-methylbenzenes. These trends between ethylene-to-propylene ratio and methanol pressure or space velocity corroborate our postulate that decreasing local methanol concentration, either by decreasing inlet methanol partial pressure or methanol space velocity, results in higher ethylene-to-propylene ratios during MTO on window-cage type materials (Fig. 1). Pursuant to the

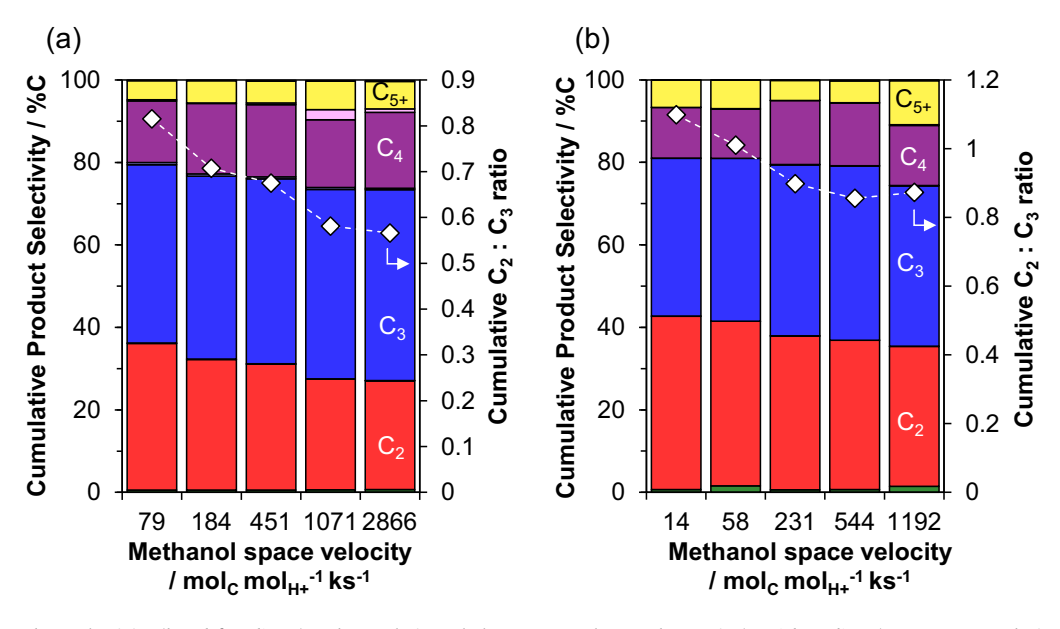


Fig. 3. Cumulative product selectivity (bar, *left ordinate*) and cumulative ethylene-to-propylene carbon ratio (\Diamond , *right ordinate*) on HSAPO-34 during methanol-to-olefins conversion at 673 K with inlet methanol pressures of (a) 30 kPa, and (b) 1 kPa when compared at similar turnover number of ~600 mol_C mol_H⁻¹. The dark- and light-shaded bars represent the olefinic and paraffinic forms, respectively, of the respective carbon group listed in the dark bars.

demonstration that distinct aromatic precursors engender ethylene and propylene in MTO catalysis [12,13,25], we sought to correlate the effect of local methanol pressure to aromatic speciation within the zeotype cavity by analyzing concentrations of entrained methylbenzenes during MTO with varying inlet methanol pressure and space velocities and detail our analysis in Section 3.2.

3.2. Effect of methanol pressure on the speciation of methylbenzenes entrained in HSAPO-34

The relative concentration of entrained methylbenzenes during methanol conversion on HSAPO-34 is compared at a similar turnover number (~1000 mol_C mol_{H+}) and plotted against inlet methanol pressure or space velocity in Figure S5.1a - c. The ratio of the molar concentration of tetra-methylbenzene relative to the sum of penta-methylbenzene and hexa-methylbenzene (TetraMB/(Pen taMB + HexaMB)) increases from 0.9 to 9.5 with inlet methanol pressure decreasing from 25.6 kPa to 0.3 kPa (Fig. S5.1a), from 1 to 2 with methanol space velocity decreasing from 2866 to 79 mol_C $mol_{H+}^{-1} ks^{-1}$ and inlet methanol pressure of ~30 kPa (Fig. S5.1b), and from 5.8 to 6.2 with methanol space velocity decreasing from 1192 to 14 mol_C $mol_{H^+}^{-1}$ ks^{-1} and inlet methanol pressure of ${\sim}1$ kPa (Fig. S5.1c). These observations suggest that decrements in local methanol concentration, either by decreasing inlet methanol pressure or space velocity, shift the distribution of entrained methylbenzenes towards lower-methylated aromatics during MTO on HSAPO-34 at a similar catalyst turnover, plausibly because of a decrease in the rate of aromatic homologation with decreasing local methanol concentration.

Fig. 4 shows that cumulative ethylene-to-propylene ratio (measured until the reaction was thermally quenched for analysis of entrained methylbenzenes) increases with increasing molar ratio of tetra-methylbenzene to the sum of penta- and hexamethylbenzene, irrespective of whether the changes in product selectivity were rendered by changes in inlet methanol pressure or space velocity. This provides further evidence for the distinct chemical origins of ethylene and propylene during MTO on HSAPO-34 where tetra-methylbenzene undergoes dealkylation reactions to form ethylene while penta- and hexa-methylbenzene undergo dealkylation reactions to yield propylene [13]. We propose that this mechanistic inference can be generalized to HSSZ-13 and HSSZ-39 to rationalize the monotonic increments in

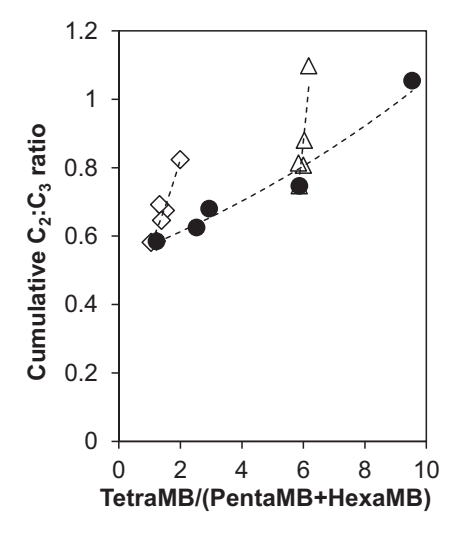


Fig. 4. Cumulative ethylene to-propylene carbon ratio on HSAPO-34 with varying inlet methanol partial pressures (\bullet), varying space velocities at 30 kPa (\diamond) and 1 kPa (\triangle) with respect to the molar ratio of tetra-methylbenzene to the sum of penta- and hexa-methylbenzene (TetraMB/(PentaMB + HexaMB)).

ethylene-to-propylene ratio with decreasing inlet methanol partial pressure and space velocity during MTO (Fig. 1).

While cumulative ethylene-to-propylene ratio generally trends with changes in the concentration of the aromatic precursor to ethylene relative to that of propylene, Fig. 4 also shows that changing inlet methanol space velocity results in changes in cumulative ethylene-to-propylene ratios without significantly altering the speciation of hydrocarbon pool (Fig. 4, diamonds and triangles). This observation implies that aromatic speciation is not a singlevalued parameter in describing trends in product selectivity during MTO on window-cage type materials, but instead, the local methanol pressure, which imposes changes in the speciation of the entrained aromatics, has additional effects on the ethylene-topropylene ratio, e.g., an overall non-zeroth order dependence of the relative formation rate of ethylene and propylene on methanol pressure. We propose that the dependence of cumulative ethyleneto-propylene ratio on methanol inlet partial pressure and space velocity (Figs. 1-3) reflects superimposed effects of local reactant concentration on instantaneous ethylene-to-propylene selectivity and the speciation of hydrocarbon pool. We sought to probe the former effect by sampling instantaneous ethylene-to-propylene ratio during transient experiments where methanol pressure was changed instantly while the hydrocarbon pool composition remained invariant within 1-2 catalyst turnovers.

3.3. Effect of methanol pressure on instantaneous ethylene-to-propylene ratio during MTO on window-cage type materials

Transient experiments in which the feed stream was switched instantly during MTO from low inlet methanol pressure (0.1-0.4 kPa) to high inlet methanol pressure (8-10 kPa) reveal that instantaneous ethylene-to-propylene ratios increase initially with reaction progress and are higher with lower inlet methanol pressure and space velocity during MTO on HSAPO-34 (Fig. S6.2, Fig. 5), HSSZ-39 (Fig. S6.3), and HSSZ-13 (Fig. S6.4), consistent with data presented in Figs. 2 and 3. The ethylene-to-propylene ratio decreases rapidly with an increase in methanol pressure and space velocity and approaches values obtained during MTO at equivalent pressures and space velocities (Fig. S6.1). The asymptotic decreasing trend in ethylene-to-propylene ratio suggests that the distribution of entrained methylbenzenes continuously evolves with turnovers and changes in local methanol concentration, providing a basis for the observed ineffectiveness in controlling cumulative ethylene-to-propylene ratio by seeding the hydrocarbon pool prior to MTO [46,47] as only the initial hydrocarbon pool speciation is altered. Further examination of the transient suggests that ethylene-to-propylene ratio decreases instantaneously with an increase in inlet methanol pressure and space velocity with changes occurring in less than 10 s (Fig. 5a) and less than 1 catalyst turnover (Fig. 5b) during which the entrained methylbenzene speciation is plausibly invariant. Similar observations are noted during transient experiments on HSSZ-13 and HSSZ-39 (Fig. S6.3 -Fig. S6.4). These data show that methanol pressure directly alters instantaneous ethylene and propylene selectivity, suggesting that (i) distinct aromatic dealkylation pathways from distinct aromatic precursors to ethylene and propylene are disparately impacted by local methanol concentration, and/or (ii) the presence of secondary pathways contributing to the formation of ethylene and propylene that vary in their dependence on methanol concentration (e.g., ethylene methylation). Ethylene methylation to propylene, however, is not a dominant secondary reaction that results in propylene formation during methanol conversion on HSAPO-34 where ethylene is regarded as a terminal product from the aromaticsbased cycle with its methylation rate being negligible during methanol conversion [10,48-50]. This inference is supported by Dahl and Kolboe [51] who co-fed ¹²C-ethylene during methanol

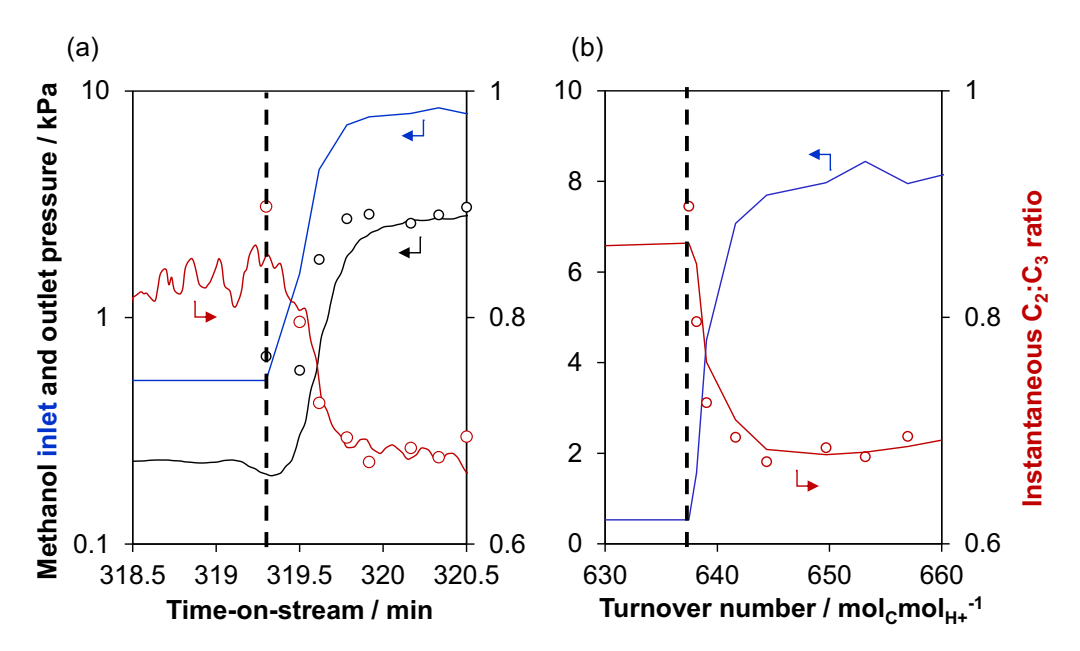


Fig. 5. Instantaneous ethylene-to-propylene carbon ratio (*right ordinate*, red, dots represent quantification from GC, lines represent quantification from MS), methanol inlet pressure (*left ordinate*, blue lines, calculated from carbon balance based on GC), and outlet methanol pressure (*left ordinate*, black, dots represent quantification from GC, lines represent quantification from MS) during methanol-to-olefins conversion on HSAPO-34 at 673 K against (a) time-on-stream, and (b) turnover number featuring the transient. Dashed lines represent onset of the transient where conditions were switched from 0.5 kPa methanol inlet pressure and space velocity of ~134 mol_C mol_{H+}⁻¹ ks⁻¹ to 8.5 kPa methanol inlet pressure and space velocity of ~1300 mol_C mol_{H+}⁻¹ ks⁻¹.

conversion on HSAPO-34 with ¹³C-methanol and observed that ¹²C-ethylene elutes without incorporation of ¹³C and that only a small amount of ¹²C is incorporated into the effluent propylene. As a result, we attribute the observed methanol pressure dependence of instantaneous ethylene-to-propylene ratio to the differences in the methanol order dependence of dealkylation rates of aromatic precursors to ethylene and propylene.

The transient experiments and the dissolution experiments presented herein suggest that methanol concentration affects ethylene-to-propylene ratio by affecting both the instantaneous ethylene and propylene selectivity via a non-zeroth order dependence on methanol concentration and the relative concentration of aromatic precursors to ethylene and propylene, rendering local methanol concentration as salient in controlling product selectivity during MTO on window-cage type materials. These results also suggest structural or chemical descriptors such as "cage-defining ring" [16] or "the interaction energy between the methylated cations and zeolite cavity" [12,25] incomplete as parameters in predicting ethylene-to-propylene ratio on window-cage type materials because the product selectivity depends not only on material parameters but is also altered in compareable or larger magnitudes by variations in local methanol pressure.

4. Conclusion

Local variations in methanol pressure, engendered by differences in process parameters such as catalyst loading, inlet methanol space velocity and partial pressure, result in changes in ethylene-to-propylene ratio during methanol conversion on window-cage type materials. Dissolution and transient experiments reveal that increase in ethylene-to-propylene ratio is correlated with decreasing local methanol concentration, which increases the instantaneous ethylene selectivity relative to the propylene selectivity and decreases the extent of homologation within entrained methylbenzenes. These results evidence and rationalize the critical role of local methanol concentration in mediating maturation of the hydrocarbon pool and product selec-

tivity during methanol conversion on window-cage type materials, and suggest structure–function metrics derived solely based on framework topology as incomplete in describing ethylene and propylene selectivity during MTO.

Declaration of Competing Interest

The authors declare that they have no known competing financial interests or personal relationships that could have appeared to influence the work reported in this paper.

Acknowledgments

We acknowledge financial support from the National Science Foundation (CBET 1701534) and Dow through the University Partnership Initiative, and Dr. Brandon Foley for valuable technical discussions.

Appendix A. Supplementary material

Supplementary data to this article can be found online at https://doi.org/10.1016/j.jcat.2021.01.015.

References

- J.Q. Chen, A. Bozzano, B. Glover, T. Fuglerud, S. Kvisle, Recent advancements in ethylene and propylene production using the UOP / Hydro MTO process, Catal. Today. 106 (2005) 103–107.
- [2] M. Yang, D. Fan, Y. Wei, P. Tian, Z. Liu, Recent progress in methanol-to-olefins (MTO) catalysts, Adv. Mater. 31 (2019) 1–15.
- [3] P. Tian, Y. Wei, M. Ye, Z. Liu, Methanol to olefins (MTO): from fundamentals to commercialization, ACS Catal. 5 (2015) 1922–1938.
- [4] B.M. Lok, C.A. Messina, R.L. Patton, R.T. Gajek, T.R. Cannan, E.M. Flanigen, Aluminophosphate molecular sieves: a new class of microporous crystalline inorganic solids, J. Am. Chem. Soc. 106 (1982) 6092–6093.
- [5] B. Vora, J.Q. Chen, A. Bozzano, B. Glover, P. Barger, Various routes to methane utilization-SAPO-34 catalysis offers the best option, Catal. Today. 141 (2009) 77–83
- [6] J.F. Haw, W. Song, D.M. Marcus, J.B. Nicholas, The mechanism of methanol to hydrocarbon catalysis, Acc. Chem. Res. 36 (2003) 317–326.

- [7] W. Song, J.F. Haw, J.B. Nicholas, C.S. Heneghan, Methylbenzenes are the organic reaction centers for methanol-to-olefin catalysis on HSAPO-34, J. Am. Chem. Soc. 122 (2000) 10726–10727.
- [8] B. Arstad, S. Kolboe, The reactivity of molecules trapped within the SAPO-34 cavities in the methanol-to-hydrocarbons reaction, J. Am. Chem. Soc. 123 (2001) 8137–8138.
- [9] B.P. Hereijgers, F. Bleken, M.H. Nilsen, S. Svelle, K.-P. Lillerud, M. Bjorgen, B.M. Weckhuysen, U. Olsbye, Product shapre selectivity dominates the methanol-to-olefins (MTO) reaction over HSAPO-34 catalysts, J. Catal. 264 (2009) 77–87.
- [10] S. Ilias, A. Bhan, Mechanism of the catalytic conversion of methanol to hydrocarbons, ACS Catal. 3 (2013) 18–31.
- [11] A. Hwang, A. Bhan, Deactivation of zeolites and zeotypes in methanol-tohydrocarbons catalysis: methanisms and circumvention, Acc. Chem. Res. 52 (2019) 2647–2656.
- [12] P. Ferri, C. Li, C. Paris, A. Vidal-Moya, M. Moliner, M. Boronat, A. Corma, Chemical and structural parameter connecting cavity architecture, confined hydrocarbon pool species, and MTO product selectivity in small-pore cagebased zeolites, ACS Catal. 9 (2019) 11542–11551.
- [13] A. Hwang, B.A. Johnson, A. Bhan, Mechanistic study of methylbenzene dealkylation in methanol-to-olefins catalysis on HSAPO-34, J. Catal. 369 (2019) 86–94.
- [14] B.V. Vora, T.L. Marker, P.T. Barger, H.R. Nilsen, S. Kvisle, T. Fuglerud, Economic route for natural gas conversion to ethylene and propylene, Stud. Surf. Sci. Catal. 107 (1997) 87–98.
- [15] S. Wilson, P. Barger, The characteristics of SAPO-34 which influence the conversion of methanol to light olefins, Microporous Mesoporous Mater. 29 (1999) 117–126.
- [16] J.H. Kang, F.H. Alshafei, S.I. Zones, M.E. Davis, Cage-defining ring: a molecular sieve structural indicator for light olefin product distribution from the methanol-to-olefins reaction, ACS Catal. 9 (2019) 6012–6019.
- [17] J. Li, Y. Wei, J. Chen, S. Xu, P. Tian, X. Yang, B. Li, J. Wang, Z. Liu, Cavity controls the selectivity: Insights of confinement effects on MTO reaction, ACS Catal. 5 (2015) 661–665.
- [18] J. Hua, X. Dong, J. Wang, C. Chen, Z. Shi, Z. Liu, Y. Han, Methanol-to-olefin conversion over small-pore DDR zeolites: tuning the propylene selectivity via the olefin-based catalytic cycle, ACS Catal. (2020) 3009–3017.
- [19] J. Chen, J. Li, Y. Wei, C. Yuan, B. Li, S. Xu, Y. Zhou, J. Wang, M. Zhang, Z. Liu, Spatial confinement effects of cage-type SAPO molecular sieves on product distribution and coke formation in methanol-to-olefin reaction, Catal. Commun. 46 (2014) 36–40.
- [20] M. Yang, B. Li, M. Gao, S. Lin, Y. Wang, S. Xu, X. Zhao, P. Guo, Y. Wei, M. Ye, P. Tian, Z. Liu, High propylene selectivity in methanol conversion over a small-pore SAPO molecular sieve with ultra-small cage, ACS Catal. 10 (2020) 3741–3749
- [21] I. Pinilla-Herrero, U. Olsbye, C. Márquez-Álvarez, E. Sastre, Effect of framework topology of SAPO catalysts on selectivity and deactivation profile in the methanol-to-olefins reaction, J. Catal. 352 (2017) 191–207.
- [22] D.M. Marcus, W. Song, L.L. Ng, J.F. Haw, Aromatic hydrocarbon formation in HSAPO-18 catalysts: cage topology and acid site density, Langmuir. 18 (2002) 8386–8391.
- [23] N. Martin, Z. Li, J. Yu, M. Moliner, A. Corma, Nanocrystalline SSZ-39 zeolite as an efficient catalyst for the methanol-to-olefin (MTO) process, Chem. Commun. 52 (2016) 6072–6075.
- [24] J.H. Kang, R. Walter, D. Xie, T. Davis, C.Y. Chen, M.E. Davis, S.I. Zones, Further studies on how the nature of zeolite cavities that are bounded by small pores influences the conversion of methanol to light olefins, ChemPhysChem. 19 (2018) 412–419.
- [25] A.A. Córma, P. Ferri, C. Li, R. Millán, J. Martínez-triguero, M. Moliner, Impact of zeolite framework composition and flexibility on MTO selectivity: confinement of diffusion?, Angew. Chem. Int. Ed. 59 (2020) 19708–19715.
- [26] T. Inui, M. Kang, Reliable procedure for the synthesis of Ni-SAPO-34 as a highly selective catalyst for methanol to ethylene conversion, Appl. Catal. A Gen. 164 (1997) 211–223.
- [27] T. Inui, S. Phatanasri, H. Matsuda, Highly selective synthesis of ethene from methanol on a novel nickel-silicoaluminophosphate catalyst, J. Chem. Soc. Chem. Commun. 20 (1990) 205–206.
- [28] T. Inui, Structure-reactivity relationships in methanol to olefin conversion on various microporous crystalline catalysts, in: Struct. Sel. Relationships Heterog. Catal., 1991, pp. 233–242.

- [29] J. Zhong, J. Han, Y. Wei, S. Xu, Y. He, Y. Zheng, M. Ye, X. Guo, C. Song, Z. Liu, Increasing the selectivity to ethylene in the MTO reaction by enhancing diffusion limitation in the shell layer of SAPO-34 catalyst, Chem. Commun. 54 (2018) 3146–3149.
- [30] J. Zhong, J. Han, Y. Wei, S. Xu, T. Sun, X. Guo, C. Song, Z. Liu, Enhancing ethylene selectivity in MTO reaction by incorporating metal species in the cavity of SAPO-34 catalysts, Chinese J. Catal. 39 (2018) 1821–1831.
- [31] H. Huang, H. Wang, H. Zhu, S. Zhang, Q. Zhang, C. Li, Enhanced ethene to propene ratio over Zn-modified SAPO-34 zeolites in methanol-to-olefin reaction, Catal. Sci. Technol. 9 (2019) 2203–2210.
- [32] W. Song, H. Fu, J.F. Haw, Supramolecular origins of product selectivity for methanol-to-olefin catalysis on HSAPO-34, J. Am. Chem. Soc. 123 (2001) 4749– 4754
- [33] S.S. Arora, D.L.S. Nieskens, A. Malek, A. Bhan, Lifetime improvement in methanol-to-olefins catalysis over chabazite materials by high-pressure H₂ cofeeds, Nat. Catal. 1 (2018) 666–672.
- [34] S.S. Arora, Z. Shi, A. Bhan, A mechanistic basis for effects of high-pressure H₂ co-feeds on methanol-to-hydrocarbons catalysis over zeolites, ACS Catal. 9 (2019) 6407–6414.
- [35] C. Baerlocher, L. McCusker, Database of Zeolite Structures, (2017). http://www.iza-structure.org/databases/ (accessed August 23, 2019).
- [36] A. Hwang, M. Kumar, J.D. Rimer, A. Bhan, Implications of methanol disproportionation on catalyst lifetime for methanol-to-olefins conversion by HSSZ-13, J. Catal. 346 (2017) 154–160.
- [37] A. Hwang, D. Prieto-Centurion, A. Bhan, Isotopic tracer studies of methanol-toolefins conversion over HSAPO-34: the role of the olefins-based catalytic cycle, J. Catal. 337 (2016) 52–56.
- [38] S.S. Arora, A. Bhan, The critical role of methanol pressure in controlling its transfer dehydrogenation and the corresponding effect on propylene-to-ethylene ratio during methanol-to-hydrocarbons catalysis on H-ZSM-5, J. Catal. 356 (2017) 300–306.
- [39] W.J.H. Dehertog, G.F. Froment, Production of light alkenes from methanol on ZSM-5 catalysts, Appl. Catal. 71 (1991) 153–165.
- [40] C.D. Chang, W.H. Lang, R.L. Smith, The conversion of methanol and other ocompounds to hydrocarbons over zeolite catalysts II. Pressure effects, J. Catal. 56 (1979) 169–173.
- [41] Ø. Mikkelsen, S. Kolboe, The conversion of methanol to hydrocarbons over zeolite H-beta, Microporous Mesoporous Mater. 29 (1999) 173–184.
- [42] S. Svelle, F. Joensen, J. Nerlov, U. Olsbye, K.P. Lillerud, S. Kolboe, M. Bjørgen, Conversion of methanol into hydrocarbons over zeolite H-ZSM-5: ethene formation is mechanistically separated from the formation of higher alkenes, J. Am. Chem. Soc. 128 (2006) 14770–14771.
- [43] S. Müller, Y. Liu, F.M. Kirchberger, M. Tonigold, M. Sanchez-sanchez, J.A. Lercher, Hydrogen transfer pathways during zeolite catalyzed methanol conversion to hydrocarbons, J. Am. Chem. Soc. 138 (2016) 15994–16003.
- [44] S. Müller, Y. Liu, M. Vishnuvarthan, X. Sun, A.C. Van Veen, G.L. Haller, M. Sanchez-Sanchez, J.A. Lercher, Coke formation and deactivation pathways on H-ZSM-5 in the conversion of methanol to olefins, J. Catal. 325 (2015) 48–59.
- [45] W. Dai, C. Wang, M. Dyballa, G. Wu, N. Guan, L. Li, Z. Xie, M. Hunger, Understanding the early stages of the methanol-to-olefin conversion on H-SAPO-34, ACS Catal. 5 (2015) 317–326.
- [46] J. Zhou, Y. Zhi, J. Zhang, Z. Liu, T. Zhang, Y. He, A. Zheng, M. Ye, Y. Wei, Z. Liu, Presituated "coke"-determined mechanistic route for ethene formation in the methanol-to-olefins process on SAPO-34 catalyst, J. Catal. 377 (2019) 153– 162
- [47] P. Bollini, A. Bhan, Improving HSAPO-34 methanol-to-olefins turnover capacity by seeding the hydrocarbon pool, ChemPhysChem. 19 (2018) 479–483.
- [48] S. Ilias, R. Khare, A. Malek, A. Bhan, A descriptor for the relative propagation of the aromatic- and olefin-based cycles in methanol-to-hydrocarbons conversion on H-7SM-5. L Catal. 303 (2013) 135–140.
- conversion on H-ZSM-5, J. Catal. 303 (2013) 135–140.

 [49] Q. Zhu, J.N. Kondo, T. Tatsumi, Microporous and mesoporous materials coreaction of methanol and ethylene over MFI and CHA zeolitic catalysts, Microporous Mesoporous Mater. 255 (2018) 174–184.
- [50] S. Svelle, O. Rønning, S. Kolboe, Kinetic studies of zeolite-catalyzed methylation reactions 1. Coreaction of [12C] ethene and [13C] methanol, J. Catal. 224 (2004) 115–123.
- [51] S.K. Dahl, M. Ivar, On the Reaction mechanism for hydrocarbon formation from methanol over SAPO34 1. Isotopic labeling studies of the co-reaction of ethene and methanol, J. Catal. 149 (1994) 458–464.